









RESEARCH ARTICLE | JUNE 20 2023

# Picosecond trion photocurrent dynamics in FAPbI<sub>3</sub> quantum dot films

Etsuki Kobiyama ; Hirokazu Tahara  ; Masaki Saruyama ; Ryota Sato ; Toshiharu Teranishi ; Yoshihiko Kanemitsu  

 Check for updates

*Appl. Phys. Lett.* 122, 252106 (2023)

<https://doi.org/10.1063/5.0154927>

 CHORUS

  
View  
Online

  
Export  
Citation

CrossMark

## Articles You May Be Interested In

Stable  $\alpha$ -FAPbI<sub>3</sub> via porous PbI<sub>2</sub> for efficient perovskite solar cells

*J. Chem. Phys.* (November 2022)

Revealing the quasiparticle electronic and excitonic nature in cubic, tetragonal, and hexagonal phases of FAPbI<sub>3</sub>

*AIP Advances* (February 2022)

Charge localization induced by reorientation of FA cations greatly suppresses nonradiative electron-hole recombination in FAPbI<sub>3</sub> perovskites: A time-domain *Ab Initio* study

*Chin. J. Chem. Phys.* (October 2020)

16 October 2023 09:42:07

 Lake Shore  
CRYOTRONICS

Cut Hall measurement time in *half*  
using an M91 FastHall™ controller



Also available as part of a tabletop system and an option for your PPMS® system

# Picosecond trion photocurrent dynamics in FAPbI<sub>3</sub> quantum dot films

Cite as: Appl. Phys. Lett. **122**, 252106 (2023); doi: [10.1063/5.0154927](https://doi.org/10.1063/5.0154927)

Submitted: 17 April 2023 · Accepted: 5 June 2023 ·

Published Online: 20 June 2023



View Online



Export Citation



CrossMark

Etsuki Kobiyama,<sup>1</sup>  Hirokazu Tahara,<sup>1,2,a)</sup>  Masaki Saruyama,<sup>1</sup>  Ryota Sato,<sup>1</sup>  Toshiharu Teranishi,<sup>1</sup>   
and Yoshihiko Kanemitsu<sup>1,a)</sup> 

## AFFILIATIONS

<sup>1</sup>Institute for Chemical Research, Kyoto University, Uji, Kyoto 611-0011, Japan

<sup>2</sup>The Hakubi Center for Advanced Research, Kyoto University, Kyoto 606-8501, Japan

<sup>a)</sup>Authors to whom correspondence should be addressed: [tahara.hirokazu.7m@kyoto-u.ac.jp](mailto:tahara.hirokazu.7m@kyoto-u.ac.jp) and [kanemitsu@scl.kyoto-u.ac.jp](mailto:kanemitsu@scl.kyoto-u.ac.jp)

## ABSTRACT

Nanocrystal quantum dot (QD) films have been highlighted as unique building blocks of optoelectronic devices due to their unique properties based on electronic interactions among close-packed QDs. Although the creation and annihilation processes of trions play important roles in optical responses of isolated QDs, their contributions to photocurrent conversion processes in QD films are unclear. Here, we studied trion dynamics in QD films by transient photocurrent measurements. We observed that the transient photocurrent signal has two decay components: a fast trion component with a lifetime shorter than 1 ns and a slow exciton component with several tens of nanoseconds. Moreover, we control the signal amplitude of the fast trion decay component by tuning extra charge doping to QDs. These results demonstrate the control of optoelectronic responses of QD films via bias electric voltage and will pave the way for QD-based ultrafast optoelectronics.

Published under an exclusive license by AIP Publishing. <https://doi.org/10.1063/5.0154927>

Colloidal semiconductor quantum dots (QDs) have attracted a great deal of attention as active materials for optoelectronic devices. One of the most significant advantages of colloidal semiconductor QDs is the easy processability by solution methods with high sample quality, e.g., almost 100% photoluminescence (PL) quantum yields at room temperature because of confined excitons.<sup>1–3</sup> In addition to excitons, three-body or four-body bound states, such as trions or biexcitons, can also be generated in QDs because the spatial confinement of photo-excited carriers leads to strong inter-carrier interactions. So far, active and outstanding research works on II–VI compound semiconductor QDs have deepened our understanding of their optical and electronic properties and dynamics of multiple excitons.<sup>4,5</sup> In addition, an ionic crystal system called metal halide perovskite emerged as a functional material for optoelectronic applications due to its superior properties.<sup>6–10</sup> In fact, halide perovskite QDs have been studied widely for applications, such as lasers,<sup>11–13</sup> light-emitting diodes (LEDs),<sup>14</sup> quantum light sources,<sup>15–17</sup> and photovoltaics,<sup>18</sup> because of the bandgap tunability based on the quantum confinement effect. Ultrafast spectroscopic methods have revealed that unique optical processes of QDs, such as low threshold lasing,<sup>19–21</sup> multiple exciton generation,<sup>22,23</sup> and coherent processes of multiple excitons,<sup>24–26</sup> can be explained with the dynamics of excitons, trions, and biexcitons. In perovskite QDs, their lowest energy levels of electrons and holes have

only twofold degeneracy due to their simple band structure. Hence, high order multiple exciton states, such as triexcitons at the low energy band, can be usually ignored. It is also known that the trion generation and recombination dynamics play essential roles in optical responses of halide perovskite.<sup>27–30</sup> Therefore, lead halide perovskite QDs are one of the best materials for studying trions and biexcitons.

Most of the previous research works for photophysics of trions and biexcitons are based on optical measurements for isolated QDs, and the contribution of trions and biexcitons to electrical properties of QD films, e.g., photocurrent conversion, remains unclear. That is because the typical timescale of electric current measurements is in order of 10 ns, which is too long to observe ultrafast dynamics of trions and biexcitons in the timescale of 10 ps ~ several hundreds of picoseconds.<sup>29,30</sup> Hence, photocurrent measurement methods with sub-nanosecond time resolution are necessary to clarify the contribution of trions to the photocurrent conversion process. In addition, as trions are positively or negatively charged excitons, their properties differ from that of charge-neutral excitons and biexcitons. Direct observation of photocurrent conversion by electric measurements helps the understanding of the relaxation dynamics and transport process of trions, which is vital for applications in photovoltaics and photodetectors.

Here, we performed transient photocurrent (TPC) measurements with sub-nanosecond time resolution to study ultrafast photocurrent

conversion dynamics in perovskite QD thin films. Due to the cubic shape of perovskite QDs, close-packed QD thin films can be fabricated easily. We found that a fast decay photocurrent signal appears in the sub-nanosecond timeframe after photoexcitation. Considering the bias voltage dependence and excitation fluence dependence of the TPC signals, we concluded that the fast decay component originates from trions. In addition, applying bias voltage on QD films leads to excess charge doping, which increases the number of trions and enhances the fast decay current component. These results are essential for understanding and applying the nonlinear photoelectric response of QD thin films.

Transient absorption (TA) measurements were performed to elucidate ultrafast optical responses of halide perovskite FAPbI<sub>3</sub> QDs (FA: formamidinium) at first. The transmission electron microscope image and x-ray diffraction pattern of the QDs show that the crystal structure was cubic, and the average edge length of the QDs was  $\sim 13$  nm (see the supplementary material). The samples were excited by a pump pulse with an energy of 3.26 eV (wavelength at 380 nm), and TA spectra were obtained with a white-light probe pulse. The details of the TA spectroscopy method are described in the supplementary material. Figure 1(a) shows a contour plot of a TA measurement where the photon fluence of the excitation pulse,  $j = 6.02 \times 10^{13}$  photons/cm<sup>2</sup>. A photobleaching signal at around 1.64 eV originates from the state filling of the lowest energy exciton level. Here, the bandgap energy of 1.64 eV is obtained from the photobleaching signal at delay time  $t = 2.5$  ns because the thermalized distribution has relaxed at this point. A strong photobleaching signal appears at delay time  $t \leq 200$  ps, and the lowest energy photobleaching signal remains afterward.

To clarify the recombination processes of trions and biexcitons, we measured the excitation fluence dependence of TA signals. Figure 1(b) shows TA signals at the photobleaching peak (1.64 eV) under different excitation intensities. Only the long lifetime component is observed in the weak excitation regime ( $j = 0.12 \times 10^{13}$  photons/cm<sup>2</sup>). In contrast, fast lifetime components are observed at early delay time under high excitation fluence ( $j \geq 0.98 \times 10^{13}$  photons/cm<sup>2</sup>), and the signal amplitudes of these components increase with excitation fluence. To obtain the lifetime of each decay component, we performed a global fitting analysis on the TA data with a triple exponential function:

$$\frac{\Delta T}{T} = A_1 \exp\left(-\frac{t}{\tau_1}\right) + A_2 \exp\left(-\frac{t}{\tau_2}\right) + A_3 \exp\left(-\frac{t}{\tau_3}\right). \quad (1)$$

Here, the parameters  $\tau_2$ ,  $\tau_3$  were treated as global parameters and the longest lifetime  $\tau_1$  was fixed to the PL lifetime of 37 ns [see Fig. S2(b) in the supplementary material]. As a result, the lifetimes of two fast decay components were obtained as  $\tau_2 = 680$  ps and  $\tau_3 = 85$  ps.

Since FAPbI<sub>3</sub> QDs have twofold degenerated band edge levels, high order multiple exciton states, such as triexcitons, do not affect the TA dynamics at the band edge level. Hence, the time constants  $\tau_1$ ,  $\tau_2$ , and  $\tau_3$  correspond to the recombination lifetimes of excitons, trions, and biexcitons, respectively.<sup>29,30</sup>

To obtain photocurrent signals by TPC measurements, we prepared QD thin films with these QDs. The surface of as-prepared QDs is covered by ligand molecules to prevent aggregation of QDs, and these ligands decrease electrical conductivity between QDs in thin films. Therefore, removing these ligands is essential for photocurrent measurement. In this study, we prepared QD films according to the sample preparation method in Ref. 31. The details are described in the supplementary material.

Figure 2(a) shows the excitation fluence dependence of the TPC signal under the applied bias voltage of 25 V, which corresponds to 50 kV/cm electric field strength. The pump pulse energy was set to 3.26 eV, as same as that of TA measurements. TPC signals consist of two decay components: a fast decay component within 2 ns after excitation and a slow decay component. For further analysis, we employed the following phenomenological model function to fit the obtained TPC signal:

$$I(t) = \left( A_{\text{long}} \exp\left(-\frac{t}{\tau_{\text{long}}}\right) + A_{\text{short}} \exp\left(-\frac{t}{\tau_{\text{short}}}\right) \right) \times \left( 1 - \text{erf}\left(\frac{t}{T}\right) \right) \times \frac{1}{2} \left( \exp\left(-\frac{t}{T_d}\right) \times \sin\left(\frac{2\pi t}{T_p}\right) + 1 \right). \quad (2)$$

Here,  $\text{erf}(x)$  is the error function and  $T$  indicates the time resolution of the instrumental response function. The third term represents the transient ringing in the TPC signals due to impedance mismatch of the components in the electric circuit, such as the device and cables.<sup>32</sup> We performed a global fitting analysis, where  $\tau_{\text{long}}$ ,  $\tau_{\text{short}}$ , and  $T$  were treated as global parameters for different excitation fluences. The details of the fitting procedure are described in the supplementary material.

The fitting result of the long decay time was  $\tau_{\text{long}} \gg 2.5$  ns, which is much larger than the time window of the measurements. Therefore,

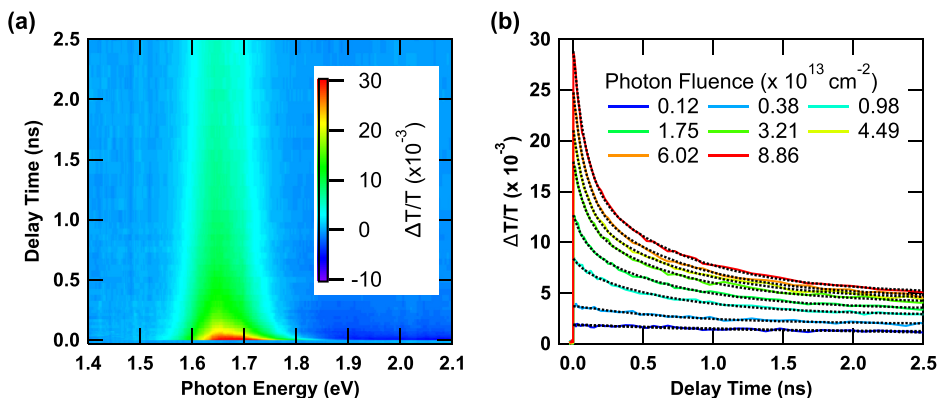
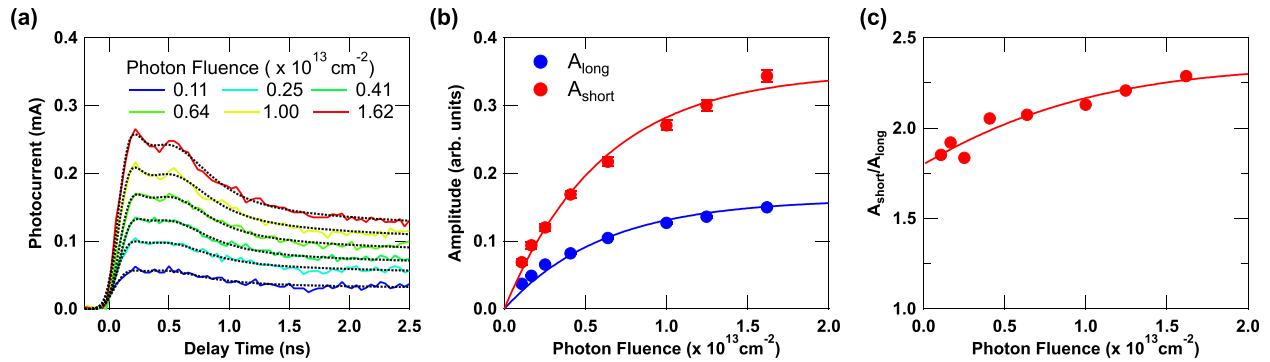


FIG. 1. (a) Two-dimensional contour plot of a TA spectrum. The excitation fluence corresponds to a photon fluence of  $6.02 \times 10^{13}$  photons/cm<sup>2</sup>. (b) TA signals at different excitation fluences. The probe energy is 1.64 eV.



**FIG. 2.** (a) TPC dynamics of a FAPbI<sub>3</sub> QD film at different excitation fluences. The broken curves represent the fitting results. (b) Excitation fluence dependence of TPC signal amplitudes of two decay components. The solid curves are the fitting results. (c) The ratio of the amplitudes as a function of excitation fluence.  $A_{\text{long}}$  and  $A_{\text{short}}$  are from the TPC measurements under the bias voltage of 25 V.

the long decay time component can be considered as constant in the TPC signals. On the other hand, the short decay time was obtained as  $\tau_{\text{short}} = 350$  ps. Since the biexciton lifetime ( $\tau_{\text{XX}} = 85$  ps) is shorter than the time resolution  $T = 110$  ps, we conclude that the short and long decay time components in the TPC signals reflect the recombination dynamics of trions and excitons, respectively. It is worth noting that the short decay time of the TPC signal is smaller than the trion lifetime obtained from the TA measurement. This result can be attributed to charge separation processes into the adjacent QDs.

Figure 2(b) shows the excitation fluence dependence of the amplitudes of two decay components. The results can be explained based on the generation process of excitons and trions. Since the TPC measurements are performed under a bias voltage, some QDs are electrically charged in TPC measurements. Excitons are generated when electrically neutral QDs absorb more than one photon. On the other hand, trions are generated when electrically charged QDs absorb more than one photon, or electrically neutral QDs absorb more than two photons.<sup>33</sup> If the average number of absorbed photons per QD is  $\langle N \rangle$  in a QD ensemble, the possibility that one QD absorbs  $N$  photons is described with the Poisson distribution.<sup>34</sup> Since  $A_{\text{long}}$  and  $A_{\text{short}}$  reflect the recombination process of excitons and trions, the excitation fluence dependencies are written as follows:

$$A_{\text{long}}(j) = A_N(1 - e^{-\sigma \cdot j}), \quad (3)$$

$$A_{\text{short}}(j) = B_C(1 - e^{-\sigma \cdot j}) + B_N(1 - e^{-\sigma \cdot j} - \sigma \cdot j \cdot e^{-\sigma \cdot j}). \quad (4)$$

Here,  $\sigma$  and  $j$  indicate the absorption cross section and excitation photon fluence. In the above equations, the product  $\sigma \cdot j$  corresponds to  $\langle N \rangle$ . The fitting results are shown as solid curves in Fig. 2(b). The obtained value of  $\sigma$  is  $(1.93 \pm 0.31) \times 10^{-13}$  cm<sup>2</sup>, which is a similar value to the previous research.<sup>35</sup> Regarding the signal amplitudes, the obtained fitting results are  $A_N = 0.18$ ,  $B_C = 0.29$ , and  $B_N = 0.06$ .  $A_{\text{long}}$  and  $A_{\text{short}}$  correspond to the number of generated excitons and trions immediately after the photoexcitation. Therefore, the sum of  $A_N$  and  $B_N$  corresponds to the number of neutral QDs, while  $B_C$  corresponds to the number of charged QDs before the photoexcitation. Since  $B_C/(B_C + A_N + B_N) = 55\%$ , more than half of QDs in the film are in the steady charged state due to the applied bias voltage.

In addition to the charging via the applied bias voltage, the excitation fluence dependence of the trion generation can be analyzed from the ratio of the amplitudes of two decay components. In Fig. 2(c), the ratio  $A_{\text{short}}/A_{\text{long}}$  is plotted as a function of photon fluence. The solid curve is the fitting result obtained by using the following equation:

$$\frac{A_{\text{short}}}{A_{\text{long}}}(j) = \frac{B_C}{A_N} + \frac{B_N(1 - e^{-\sigma \cdot j} - \sigma \cdot j \cdot e^{-\sigma \cdot j})}{A_N(1 - e^{-\sigma \cdot j})}. \quad (5)$$

The first term corresponds to the contribution of the electrically charged QDs to the trion generation: more than one photon absorption by electrically charged QDs. On the other hand, the second term corresponds to the multiple photon absorption by electrically neutral QDs. Since the first term is constant, the gradual increase in the ratio indicates the increasing contribution of the multiple photon absorption process by electrically neutral QDs. As the highest limit of the ratio is  $B_C/A_N + B_N/A_N$ , the fraction of the neutral QDs' contribution can increase up to  $(B_N/A_N)/(B_C/A_N + B_N/A_N) = B_N/(B_C + B_N) = 17\%$  in the strong photoexcitation conditions. This value is significantly smaller than the contribution of the steady charging by the applied bias voltage,  $B_C/(B_C + B_N) = 83\%$ . Thus, applying bias voltage can be an efficient way to tune the trion generation ratios.

Figure 3 shows the TPC dynamics under different bias voltages of 5, 15, and 25 V, which correspond to the electric field strength of 10, 30, and 50 kV/cm, respectively. Here, the excitation fluence is  $j = 0.49 \times 10^{13}$  photons/cm<sup>2</sup>, which corresponds to  $\langle N \rangle = 0.95$ . In Fig. 3(a), the slow decay component shows a small increase, while the fast decay component increases more drastically. This result indicates that the trion contribution gets pronounced with the increase in the bias voltage. The signal amplitudes of trion and exciton components,  $A_{\text{short}}$  and  $A_{\text{long}}$ , and the ratio of these amplitudes,  $A_{\text{short}}/A_{\text{long}}$ , are plotted in Figs. 3(b) and 3(c). The ratio shows a linear increase with the applied bias voltage and reaches 1.90 at 25 V. The ratio under zero bias voltage was obtained as  $1.01 \pm 0.33$  by extrapolating the experimental results. Thus, the bias voltage of 25 V enhances the ratio by 1.88 times. This enhancement indicates that trions are generated with the assistance of carrier doping via applying the bias voltage.

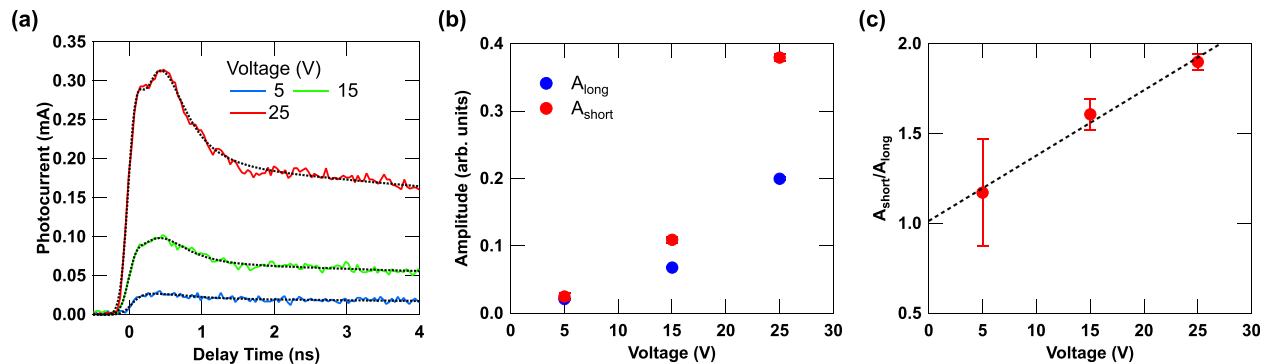


**FIG. 3.** (a) TPC dynamics of the FAPbI<sub>3</sub> QD film under different bias voltages. The broken lines represent the fitting results. The bias voltage dependence of (b) the TPC signal amplitudes and (c) the ratio of the amplitudes.  $A_{\text{long}}$  and  $A_{\text{short}}$  indicate the amplitudes of the long and short decay time components, respectively.

In conclusion, we studied the photocurrent conversion process in FAPbI<sub>3</sub> QD films using TA and TPC measurements. Based on the comparison between the TA and TPC dynamics, we clarified that short and long decay time components of TPC signals reflect the recombination processes of trions and excitons, respectively. In addition, we demonstrated that the TPC dynamics can be controlled by applying bias voltage on a QD film and doping extra charges on QDs. These results provide important insights into the ultrafast operation of QD-based photodetector. Moreover, steady charging of QDs by carrier doping from electrodes has potential applications in low-threshold lasers by trion generation and ultrafast electronics with tunable electrical or laser pulse widths.<sup>20,36</sup>

See the supplementary material for fabrication and characterization of the samples, spectroscopic measurements, and transient photocurrent signal analysis.

Part of this work was supported by the JSPS KAKENHI (Grant Nos. JP19H05465 and JP22H01990) and JST CREST (Grant No. JPMJCR21B4).

## AUTHOR DECLARATIONS

### Conflict of Interest

The authors have no conflicts to disclose.

### Author Contributions

**Etsuki Kobiyama:** Data curation (lead); Formal analysis (lead); Investigation (lead); Writing – original draft (lead). **Hirokazu Tahara:** Formal analysis (equal); Investigation (equal); Methodology (equal); Writing – review & editing (equal). **Masaki Saruyama:** Resources (lead). **Ryota Sato:** Resources (supporting). **Toshiharu Teranishi:** Resources (supporting). **Yoshihiko Kanemitsu:** Supervision (equal); Writing – review & editing (equal).

### DATA AVAILABILITY

The data that support the findings of this study are available from the corresponding authors upon reasonable request.

## REFERENCES

- <sup>1</sup>Y. Shirasaki, G. J. Supran, M. G. Bawendi, and V. Bulović, “Emergence of colloidal quantum-dot light-emitting technologies,” *Nat. Photonics* **7**(1), 13–23 (2013).
- <sup>2</sup>L. Protesescu, S. Yakunin, M. I. Bodnarchuk, F. Krieg, R. Caputo, C. H. Hendon, R. X. Yang, A. Walsh, and M. V. Kovalenko, “Nanocrystals of cesium lead halide perovskites (CsPbX<sub>3</sub>, X = Cl, Br, and I): Novel optoelectronic materials showing bright emission with wide color gamut,” *Nano Lett.* **15**(6), 3692–3696 (2015).
- <sup>3</sup>D. A. Hanifi, N. D. Bronstein, B. A. Koscher, Z. Nett, J. K. Swabeck, K. Takano, A. M. Schwartzberg, L. Maserati, K. Vandewal, Y. van de Burgt, A. Salleo, and A. P. Alivisatos, “Redefining near-unity luminescence in quantum dots with photothermal threshold quantum yield,” *Science* **363**(6432), 1199–1202 (2019).
- <sup>4</sup>J. M. Pietryga, Y. S. Park, J. Lim, A. F. Fidler, W. K. Bae, S. Brovelli, and V. I. Klimov, “Spectroscopic and device aspects of nanocrystal quantum dots,” *Chem. Rev.* **116**(18), 10513–10622 (2016).
- <sup>5</sup>H. Jung, N. Ahn, and V. I. Klimov, “Prospects and challenges of colloidal quantum dot laser diodes,” *Nat. Photonics* **15**(9), 643–655 (2021).
- <sup>6</sup>S. D. Stranks and H. J. Snaith, “Metal-halide perovskites for photovoltaic and light-emitting devices,” *Nat. Nanotechnol.* **10**(5), 391–402 (2015).
- <sup>7</sup>B. R. Sutherland and E. H. Sargent, “Perovskite photonic sources,” *Nat. Photonics* **10**(5), 295–302 (2016).
- <sup>8</sup>Y. Kanemitsu, “Luminescence spectroscopy of lead-halide perovskites: Materials properties and application as photovoltaic devices,” *J. Mater. Chem. C* **5**(14), 3427–3437 (2017).
- <sup>9</sup>Y. Yamada, T. Yamada, L. Q. Phuong, N. Maruyama, H. Nishimura, A. Wakamiya, Y. Murata, and Y. Kanemitsu, “Dynamic optical properties of CH<sub>3</sub>NH<sub>3</sub>PbI<sub>3</sub> single crystals as revealed by one- and two-photon excited photoluminescence measurements,” *J. Am. Chem. Soc.* **137**(33), 10456–10459 (2015).
- <sup>10</sup>Z. K. Tan, R. S. Moghaddam, M. L. Lai, P. Docampo, R. Higler, F. Deschler, M. Price, A. Sadhanala, L. M. Pazos, D. Credgington, F. Hanusch, T. Bein, H. J. Snaith, and R. H. Friend, “Bright light-emitting diodes based on organometal halide perovskite,” *Nat. Nanotechnol.* **9**(9), 687–692 (2014).
- <sup>11</sup>S. Yakunin, L. Protesescu, F. Krieg, M. I. Bodnarchuk, G. Nedelcu, M. Humer, G. De Luca, M. Fiebig, W. Heiss, and M. V. Kovalenko, “Low-threshold amplified spontaneous emission and lasing from colloidal nanocrystals of caesium lead halide perovskites,” *Nat. Commun.* **6**(1), 8056 (2015).
- <sup>12</sup>G. Yumoto, H. Tahara, T. Kawawaki, M. Saruyama, R. Sato, T. Teranishi, and Y. Kanemitsu, “Hot biexciton effect on optical gain in CsPbI<sub>3</sub> perovskite nanocrystals,” *J. Phys. Chem. Lett.* **9**(9), 2222–2228 (2018).
- <sup>13</sup>E. Kobiyama, H. Tahara, R. Sato, M. Saruyama, T. Teranishi, and Y. Kanemitsu, “Reduction of optical gain threshold in CsPbI<sub>3</sub> nanocrystals achieved by generation of asymmetric hot-biexcitons,” *Nano Lett.* **20**(5), 3905–3910 (2020).

- <sup>14</sup>J. Song, J. Li, X. Li, L. Xu, Y. Dong, and H. Zeng, "Quantum Dot Light-Emitting Diodes Based on Inorganic Perovskite Cesium Lead Halides (CsPbX<sub>3</sub>)," *Adv. Mater.* **27**(44), 7162–7167 (2015).
- <sup>15</sup>H. Utzat, W. Sun, A. E. K. Kaplan, F. Krieg, M. Ginterseder, B. Spokoyny, N. D. Klein, K. E. Shulenberger, C. F. Perkinson, M. V. Kovalenko, and M. G. Bawendi, "Coherent single-photon emission from colloidal lead halide perovskite quantum dots," *Science* **363**(6431), 1068–1072 (2019).
- <sup>16</sup>Y.-S. Park, S. Guo, N. S. Makarov, and V. I. Klimov, "Room temperature single-photon emission from individual perovskite quantum dots," *ACS Nano* **9**(10), 10386–10393 (2015).
- <sup>17</sup>Y. Lv, C. Yin, C. Zhang, W. W. Yu, X. Wang, Y. Zhang, and M. Xiao, "Quantum interference in a single perovskite nanocrystal," *Nano Lett.* **19**(7), 4442–4447 (2019).
- <sup>18</sup>S. S. Mali, C. S. Shim, and C. K. Hong, "Highly stable and efficient solid-state solar cells based on methylammonium lead bromide (CH<sub>3</sub>NH<sub>3</sub>PbBr<sub>3</sub>) perovskite quantum dots," *NPG Asia Mater.* **7**(8), e208 (2015).
- <sup>19</sup>Z. Qin, C. Zhang, L. Chen, T. Yu, X. Wang, and M. Xiao, "Electrical switching of optical gain in perovskite semiconductor nanocrystals," *Nano Lett.* **21**(18), 7831–7838 (2021).
- <sup>20</sup>K. Wu, Y. S. Park, J. Lim, and V. I. Klimov, "Towards zero-threshold optical gain using charged semiconductor quantum dots," *Nat. Nanotechnol.* **12**(12), 1140–1147 (2017).
- <sup>21</sup>Y. Wang, M. Zhi, Y. Q. Chang, J. P. Zhang, and Y. Chan, "Stable, ultralow threshold amplified spontaneous emission from CsPbBr<sub>3</sub> nanoparticles exhibiting trion gain," *Nano Lett.* **18**(8), 4976–4984 (2018).
- <sup>22</sup>C. de Weerd, L. Gomez, A. Capretti, D. M. Lebrun, E. Matsubara, J. Lin, M. Ashida, F. C. M. Spoor, L. D. A. Siebbeles, A. J. Houtepen, K. Suenaga, Y. Fujiwara, and T. Gregorkiewicz, "Efficient carrier multiplication in CsPbI<sub>3</sub> perovskite nanocrystals," *Nat. Commun.* **9**(1), 4199 (2018).
- <sup>23</sup>M. Li, R. Begum, J. Fu, Q. Xu, T. M. Koh, S. A. Veldhuis, M. Grätzel, N. Mathews, S. Mhaisalkar, and T. C. Sum, "Low threshold and efficient multiple exciton generation in halide perovskite nanocrystals," *Nat. Commun.* **9**(1), 4197 (2018).
- <sup>24</sup>H. Tahara, M. Sakamoto, T. Teranishi, and Y. Kanemitsu, "Harmonic quantum coherence of multiple excitons in PbS/CdS core-shell nanocrystals," *Phys. Rev. Lett.* **119**(24), 247401 (2017).
- <sup>25</sup>H. Tahara, M. Sakamoto, T. Teranishi, and Y. Kanemitsu, "Quantum coherence of multiple excitons governs absorption cross-sections of PbS/CdS core-shell nanocrystals," *Nat. Commun.* **9**(1), 3179 (2018).
- <sup>26</sup>H. Tahara, M. Sakamoto, T. Teranishi, and Y. Kanemitsu, "Collective enhancement of quantum coherence in coupled quantum dot films," *Phys. Rev. B* **104**(24), L241405 (2021).
- <sup>27</sup>Y. Kanemitsu, "Trion dynamics in lead halide perovskite nanocrystals," *J. Chem. Phys.* **151**(17), 170902 (2019).
- <sup>28</sup>G. Yumoto and Y. Kanemitsu, "Biexciton dynamics in halide perovskite nanocrystals," *Phys. Chem. Chem. Phys.* **24**(37), 22405–22425 (2022).
- <sup>29</sup>N. S. Makarov, S. Guo, O. Isaienko, W. Liu, I. Robel, and V. I. Klimov, "Spectral and dynamical properties of single excitons, biexcitons, and trions in cesium-lead-halide perovskite quantum dots," *Nano Lett.* **16**(4), 2349–2362 (2016).
- <sup>30</sup>N. Yarita, H. Tahara, T. Ihara, T. Kawawaki, R. Sato, M. Saruyama, T. Teranishi, and Y. Kanemitsu, "Dynamics of charged excitons and biexcitons in CsPbBr<sub>3</sub> perovskite nanocrystals revealed by femtosecond transient-absorption and single-dot luminescence spectroscopy," *J. Phys. Chem. Lett.* **8**(7), 1413–1418 (2017).
- <sup>31</sup>A. Swarnkar, A. R. Marshall, E. M. Sanehira, B. D. Chernomordik, D. T. Moore, J. A. Christians, T. Chakrabarti, and J. M. Luther, "Quantum dot-induced phase stabilization of CsPbI<sub>3</sub> perovskite for high-efficiency photovoltaics," *Science* **354**(6308), 92–95 (2016).
- <sup>32</sup>J. Gao, S. C. Nguyen, N. D. Bronstein, and A. P. Alivisatos, "Solution-processed, high-speed, and high-quantum-efficiency quantum dot infrared photodetectors," *ACS Photonics* **3**(7), 1217–1222 (2016).
- <sup>33</sup>S. Nakahara, K. Ohara, H. Tahara, G. Yumoto, T. Kawawaki, M. Saruyama, R. Sato, T. Teranishi, and Y. Kanemitsu, "Ionization and neutralization dynamics of CsPbBr<sub>3</sub> perovskite nanocrystals revealed by double-pump transient absorption spectroscopy," *J. Phys. Chem. Lett.* **10**(16), 4731–4736 (2019).
- <sup>34</sup>V. I. Klimov, "Optical nonlinearities and ultrafast carrier dynamics in semiconductor nanocrystals," *J. Phys. Chem. B* **104**(26), 6112–6123 (2000).
- <sup>35</sup>H.-H. Fang, L. Protesescu, D. M. Balazs, S. Adjokatse, M. V. Kovalenko, and M. A. Loi, "Exciton recombination in formamidinium lead triiodide: Nanocrystals versus thin films," *Small* **13**(32), 1700673 (2017).
- <sup>36</sup>O. V. Kozlov, Y. Park, J. Roh, I. Fedin, T. Nakotte, and V. I. Klimov, "Sub-single-exciton lasing using charged quantum dots coupled to a distributed feedback cavity," *Science* **365**(6454), 672–675 (2019).